Rotating Molten Metallic Drops and Their Applications for Surface Tension Measurements

Won-Kyu Rhim and Takehiko Ishikawa*
Jet Propulsion Laboratory, California Institute of Technology,
4800 Oak Grove Drive, Pasadena, California 91109, USA

(March 1998)

*On leave from the National Space Development Agency of Japan

Abstract

Shapes and stability of rotating molten metal drops carrying net surface electric charges are experimentally investigated, and the feasibility of measuring surface tension based on drop rotation is examined. Molten aluminum and tin drops were levitated in a high vacuum by controlling applied electric fields, and they were systematically rotated by applying torques generated by rotating magnetic field. As the drops gained angular momentum gradually (or step by sptep) from their static states, the their shapes evolved along the axi-symmetric branch until the bifurcation point was reached at which transformation from axi-symmetric to tri-axial shape took place With the assumption of 'effective surface tension' which includes the effect of reduced surface tension due to the surface charges, the results agree quantitatively well with the Brown and Scriven's prediction. The normalized rotation frequencies at the bifurcation point agreed well with the predicted value, 0.559, within 2 %. Also discussed in this paper are some anomalous results which have been observed under specific rotating conditions.

1. Introduction

As eloquently stated by Swiatecki [1], the problem of a rotating drop held together by a surface tension is 'a special case of a single mathematical structure which embraces in a unified manner the equilibrium of rotating masses representing at one extreme idealized atomic nuclei, at the other idealized heavenly bodies, and covering in between engineering applications in weightless space laboratories'. Since Rayleigh's[2] initial calculation of axi-symmetric shapes of rotating drops, the theoretical predictions have been brought to a rare degree of accuracy by Chandrasekhar[3], and more recently by Brown and Scriven[4] in their numerical studies on the stability of various equilibrium shapes of uncharged drops. Over the last decade there have been several efforts to experimentally verify these predictions. Rhim, Chung and Elleman[5] performed the experiment in the ground-base using charged drops levitated in an electrostatic field while rotating the drop using acoustic torque, obtaining an n=2 bifurcation point close to the theoretical prediction. However, the drops carrying electric charges casted some doubt as to the validity of the system to verify the theory which assumes electrically neutral drops. Biswas, Leung and Trinh[6] studied the bifurcation of acoustically levitated and rotated drops on the ground base. Using acoustally squeezed drops (in static state) they obtained results which seemed to corroborate results which were observed during the 1986 Space experiments[7]. Recently Wang, Anilkumar, Lee and Lin repeated their experiment with improved equipment in the Space Shuttle USML-1. Using spherical drops of silicone oil and glycerine/water mixture they obtained results which closely agreed with the prediction as long as the drops rotated satisfying the solidbody rotation condition. All of above experiments used non-metallic liquids. Also the techniques and the environment surrounding drops cannot be directly transfered to many molten metallic drops whose properties are desperately needed in order to understand their solidification processes.

This paper describes the first attempt of using molten metal drops to confirm the predicted drop rotation behavior and to apply it for a new way of measuring surface tension. For low viscosity liquids, the drop oscillation technique is an adequate non-contact surface

tension measurement technique. However, for high viscosity liquids where drop oscillations cannot be induced, a new non-contact technique is needed. For example, viscosities of glass forming alloy liquids increase nearly 14 orders magnitude before they their glass transition temperatures are reached. In addition we will present an unexpected result in rotating molten tin, in which separating isotopes are believed to be the cause.

2. Experimental Apparatus and Approach

The basic approach of this experiment was to apply a steady (or step by step) low level torques to a molten metallic drop levitated in a high vacuum. The High Temperature Electrostatic Levitator (HTESL) at Jet Propulsion Laboratory levitates a sample 1 to 3 mm in diameter between a pair of parallel disk electrodes which are spaced about 12 mm (Fig. 1). The electric field between these two electrodes generates a sufficient electrostatic force on a charged sample which can cancel the downward gravitational force. The four small side electrodes around the bottom electrode control the sample position along horizontal direction. The main position control voltage is connected to the upper electrode, while the bottom electrode is electrically grounded through an ac voltage source. This ac voltage source superimposes an oscillating electric field on the levitation field for the purpose of inducing resonant oscillations on a levitated drop. The four coils positioned around the top electrode produce horizontal magnetic field which rotates at an appropriate frequency (400 Hz in the present experiment) in order to induce sample rotation. The electrode assembly is housed by a stainless steel chamber which is typically evacuated to ~10^{-8} torr. Samples are heated using a xenon arc lamp. Detailed description of the HTESL is given in an earlier publication[8].

The experiments were conducted using high purity aluminum and tin samples at approximately 25 K above respective melting points. Once a levitated sample was fully molten, it was further outgased (removing volatile impurities) by raising the temperature approximately 200 K above melting points. Once the sample temperature was lowered to the predetermined operational temperature, it was kept constant. At the operational temperature, the sample

position instability was minimized by adjusting servo parameters until the magnified drop viewed on a TV monitor looked very quiescent. Once such initial condition was prepared, the resonance frequency at n = 2 mode was measured as it was induced by applying a low level ac electric field. Following the measurement, the ac field was turned off, and the sample rotation was initiated by applying rotating magnetic field at a preset amplitude and frequency.

Four identical coils were wound to produce the rotating magnetic field. Each coil was wound on a glass spool (28 mm in length, and ~ 8 mm in diameter) with 28 gauge insulated copper wire. Spools were made out of silica glass for electrical insulation purpose since the coils were to be mounted in the proximity of high voltage electrode (the top electrode). When 400 turns were wound on a spool, the coil's inductance and resistance were ~ 34 mH and ~ 5.3 ohm, respectively. When a soft iron core (0.25 inch in diameter, and 2.25 inches in length) was slid through a coil, approximately 3.2 mili-Tesler of magnetic field could be produced at an end of the coil carrying 140 mA. These four coils were mounted on top of the top electrode with iron cores imbedded in it increase the magnetic field at the sample position (see Fig. 1). Installing the coils on the top electrode, although it involved less than a trivial insulation problem, was chosen since the space below the bottom electrode was fully occupied by the sample storage/retrieval carousel.

The four coil assembly so mounted were driven by the current generator unit as shown in Fig. 2. A dual channel signal generator (HP 3326A) produced two low level sinusoidal signals with 90 degrees phase difference. We found that 400 Hz was adequate frequency for the present experiment. These two signals were then amplified by two separate amplifiers (HP 6825A) before connected to a switch box. This switch box controls the current which is going through each coil to produce various magnetic field: (i) an OFF switch cuts off currents from all four coils, (ii) a CLOCKWISE switch wires the coils so that the horizontal magnetic field seen by the sample rotates in the clockwise direction, (iii) a C-CLOCKWISE reverses the field rotation from clockwise to counter-clockwise direction, and (iv) an additional switch not shown in Fig. 2 is a VERTICAL switch which connects the coils in such a way to produce

magnetic field along vertical direction. Vertical magnetic field can damp sample rotation if its rotational axis is is in horizontal plane. Both the CLOCKWISE and C-CLOCKWISE modes can be used either to accelerate or decelerate the sample around vertical axis depending upon sample's rotational state. The currents flowing through each set of coils were monitored by voltages across 1 ohm resistors.

The basic principle of the present sample rotation mechanism is essentially same as the asynchronous induction motor. The four coil assembly works as the stator while the levitated sample serving as a rotor. According to the principle of induction motor[9, 10], if an ac voltage E_1 at frequency ω_s is applied to the stator having resistance R_1 and inductance L_1, the torque τ experienced by the rotor (having its own resistance R_2 and inductance L_2) rotating at an instantaneous rotation frequency ω is given by

$$\tau = \frac{\omega_s E_1^2}{R_1^2 + \omega_s^2 L_1^2}\left(\frac{sR_2}{R_2^2 + s^2 L_2^2}\right), \tag{1}$$

where

$$s \equiv \frac{\omega_s - \omega}{\omega_s}. \tag{2}$$

The Eq. (1) was put on a test using a levitated aluminum sphere by measuring the torque for a given input parameters as a function of sample rotation frequency. Fig.3 shows that at a fixed stator current the torque is a linear function of s, therefore, linearly proportional to the instantaneous sample rotational frequency. This means that the relationship $R_2^2 >> s^2L^2$ is well satisfied in Eq. (1), transforming the equation to a simpler form:

$$\tau = \left(\frac{\omega_s E_1^2}{R_1^2 + \omega_s^2 L_1^2}\right)\frac{1}{R_2}\left(1 - \frac{\omega}{\omega_s}\right). \tag{3}$$

Accurate measurements of sample rotation frequency is important for accurate determination of torque imparted to the sample. In our experiment, a He-Ne laser beam was directed to the sample and the reflected beam was detected by a silicon photo-detector. The

output voltage of the detector was amplified and digitized to get Fourier power spectrum using a micro-computer. Such power spectrum showed peaks at all harmonics of the sample rotation frequency. Such power spectrum only serves as a coarse indicator of the rotation frequency. More precise detection of sample rotation was done by exploiting strobe effect created by a TV monitor. Regular monitors have 30 Hz frame rate (or 60 Hz field rate). A CCD camera operated at the 0.001 second shutter speed was mounted on a tele-microscope to produce a magnified sample image on a TV screen. Whenever the sample rotation rate approached one of the harmonic or sub harmonic frequencies of the 60 Hz field rate, seemingly static image was observable. Such a stroboscopic approach assisted by the frequency information obtained by the power spectrum display allowed us precise determination of sample rotation frequency without ambiguity.

3. Experiment on solid body rotation.

For drop rotation experiments we chose a high purity aluminum and a tin samples. All parameters relevant to these samples and experimental conditions are as shown in Table I. Each rotation experiment was initiated by applying the rotating magnetic field to the sample and by video-recording the drop side view on a video tape. Drop rotation frequnecy was was also recorded overlayed on the video recording.

As the drop started rotating, slightly prolate initial shape turned progressively oblate spheroid, and this trend continued until they reached a critical point, the bifurcation point, where the drops turned into triaxial ellipsoidal shape. From this point on, as a result of rapidly increasing moment of inertia, the drop rotation frequency started to decrease even though the drop gained more angular momentum. This behavior is in accordance with the earlier experimental results on rotating charged water drops on the ground base[5]. This result is also in accorance with their rotating glycerine/water mixture (and also with their silicon oil) drop experiments in the Space Shuttle by Wang et al.[11] except that their drops were electrically neutral and the initial drop shapes were rather slightly oblate as a result of applied acoustic

pressure. Fig. 4 shows the evolution of normalized drop dimension, R_{max}/R_o, versus the normalized rotation frequency, $\omega_{rot}/\omega_{osc}$, where R_{max} and R_o are the maximum radius of the rotating drop and the radius of spherical shape, respectively. The drop rotation frequency $\omega_{rot.}$ is normalized by its own oscillation frequency ω_{osc} (n = 2 mode) measured at the non-rotating state. Also plotted in this figure is the theoretical result calculated by Brown and Scriven[4] showing initially axi-symmetric drop shape branching out to two lobed, three lobed, or four lobed drop shape at the different critical frequencies. In reality, however, the two-lobe branch is the one to which the shape transformation takes place. Transition between these to branches were reversible as long as the applied torque level was kept sufficiently low to ensure solid body rotation. As one can see in the figure, the experimental points of both the aluminum and tin drops follow the theoretical curve within 2%. We observe that the data points along the axi-symmetric branch are slightly below the theoretical curve. This is caused due to the initial oblate shape of the drop at non-rotating state. The observed bifurcation point also agrees with predicted value, $\omega_{rot}/\omega_{osc} = 0.559$, within 2 %.

In a separate experiment using a different aluminum drop (see Table II), basically the same result as Fig. 4 was obtained as shown in Fig. 5. The data points closely followed the predicted axi-symmetric branch except slight over shooting beyond the predicted bifurcation point ($\omega_{rot}/\omega_{osc} = 0.559$). Fig. 6 shows the side views of the rotating aluminum drop corresponding to data points indicated in Fig. 5. The points **a**, **b**, **c**, and **d** correspond to axi-symmetric shapes. However, at the point **d**, a quick transition took place from an axi-symmetric to triaxial ellipsoidal shape (to the point **e** on the two-loved branch). With further gaining of angular momentum, the drop shape changed to the point **f**. When the angular momentum was reduced by small step by step, the drop followed the two-loved branch down to the predicted bifurcation point. Most likely the overshooting beyond the bifurcation point was caused by the high torque which prevented the drop from reaching solid-body rotation condition. In fact, similar overshooting behavior was also observed by Wang et al. in a Space

experiment when an excessive level of acoustic torque was applied to a glycerol/water drop[11].

An unexpected result was observed when a rotating experiment was performed with a molten tin drop, with 39.8 mg in mass. Again the drop was rotated at a high torque level which produced overshooting beyond the predicted bifurcation point (see Fig. 7). The drop angular momentum was further increased to a point where R_{max}/R_o was approximately 1.6. Applied torque was turned off at this point and allowed the drop to rotate freely (in the frictionless vacuum) for the next two hours at the same temperature. Now, when the drop angular momentum was slowly reduced under the influence of negative torque, surprisingly the drop shape evolved following a quite different path away from the theoretical branches. In fact, the drop shape remained as triaxial ellipsoidal all the way down to non-rotating state, completely by-passing the axi-symmetric branch. When the rotation frequency was slowed down to approximately 10 Hz, the drop (originally with its longest axis perpendicular to the vertical rotation axis) became unstable, and it eventually lined its longest axis along the gravity field as the angular momentum was further reduced. The final shape and orientation of the drop is shown in Fig. 8. Cause of this anomaly is not understood at this moment. Present authors only speculate that probably cause might be isotopes in the rotating tin drop separating under the influence of centrifugal force, although we failed to confirm this using the Secondary Ion Mass Spectrometer. Tin has seven highly abundant isotopes between ^{116}Sn (14.53 %) and ^{124}Sn (5.79 %), among which ^{120}Sn (32.59 %) being the most abudant isotope. Anomaly similar to tin samples could not be observed in molten aluminums. In natural aluminum, ^{27}Al is essentially the only isotope. If we consider a sphere, 1.5 mm in radius, that is rotating at 50 Hz, the difference in centrifugal acceleration between the center and the surface of the drop is as much as 15 times the Earth gravitational acceleration. More systematic experiments and some theoretical modeling are required before understanding of such behavior can be obtained.

4. Measurement of Surface Tension by Drop Rotation

In this section the possibility of measuring surface tension by drop rotating will be investigated. For low viscosity liquids, measurement of resonant oscillation of a levitated drop is an accurate means of extracting its surface tension[12, 13]. However, the accuracy of this method decreases as the damping constant of free oscillation becomes shorter due to increasing viscosity.

If a drop rotates according to the theoretical curve as shown in Fig.4, one can determine the oscillation frequency, ω_{osc}, at any point of the curve, if the shape parameter, R_{max}/R_o, and the rotation frequency, ω_{rot}, are known. We notice that liquid viscosity does not play any role in the theory of rotating drops as long as the drop can reach the condition of solid body rotation. Higher viscosity will only help bringing the solid-body condition quickly. A proposal of measuring surface tension using drop rotation was made early on by Elleman et al.[14]. Since the drop rotation frequency of an axi-symmetric drop is difficult to measure if the drop surface is extremely uniform, the drop rotation frequency should be made on the triaxial branch close to the bifurcation point. Since $\omega_{rot}/\omega_{osc}= 0.559$ at the bifurcation point, and ω_{rot} can be measured, ω_{osc} is determined. This approach for surface tension measurement should be applicable to metallic melts regardless their viscosity if the solid-body rotation condition is respected.

In this section we intend to sytematically verify this surface tension measurement approach using a molten tin and and an aluminum drop (see Table II). Since both drops showed surface structure caused by oxide layers, we could also measure the drop rotation frequencies along the axi-symmetric branch using the rotation detection method described in a previous section. To obtain a more amplified view of drop shape changes, the axi-symmetric values of the two rotating melts and the theoretical points were plotted in Fig.9 in terms of R_{max}/R_{min} instead of R_{max}/R_o, where R_{min} is the vertical dimension of rotating drop. (Aluminum data in Fig. 9 are the same set of data shown in Fig. 5.) At their static states ($\omega_{rot.}$ = 0), both drops showed slight elongations along vertical direction. We searched for

appropriate multiplication factors (one for the aluminum and one for the tin, respectively), which would make $R_{max}/R_{min} = 1$ at $\omega_{rot}/\omega_{osc} = 0$, and apply them to respective set of data as shown in Fig. 10. As one can see, agreement between these two sets of data is very good. Since aluminum data showed very close agreement with the theory as demonstrated in Fig. 5, let us assume that the best fit curve to axi-symmetric points of aluminum data overlaps the theoretical curve if it is plotted in the R_{max}/R_{min} scale. The fitting curve can be expressed by

$$R_{max}/R_{min} = 1 - 6.655 \times 10^{-2} F + 1.663 F^2 - 2.669 F^3 + 4.445 F^4 \qquad (4)$$

where $F = \omega_{rot}/\omega_{osc}$. For every experimental data in Fig. 10, R_{max}/R_{min} and $\omega_{rot.}$ are known, therefore, ω_{osc} can be determined if Eq. (4) is used to find $\omega_{rot}/\omega_{osc}$ corresponding to R_{max}/R_{min} of a given data point. $\omega_{osc.}$ values so obtained from every tin data shown in Fig. 10 are plotted against $\omega_{rot}/\omega_{osc}$ in Fig. 11. Also indicated in the figure is the actual oscillation frequency which was directly measured from the same tin drop by inducing a resonant oscillation at n = 2 mode. As one can see from the figure, the oscillation frequencies extracted from tin data at lower rotation frequencies show larger uncertainties, while those which correspond to higher rotational frequency rapidly converge to the actual oscillation frequency within +/-2 % (which corresponds to +/- 2 Hz for the tin used). The oscillation frequency directly measured on the molten tin drop are usually reproducable within 0.5 Hz. Also noticable in Fig. 11 is that the oscillation frequency determined by the overshot points show rather strong divergence from the actual frequency.

Under the assumption of uniform distribution of surface charge, ω_{osc} so obtained is related to the surface tension of the liquid σ by[12]

$$\omega_{osc.}^2 = \frac{8\sigma}{\rho r_o^3}\left(1 - \frac{Q_s^2}{64\pi^2 r_o^3 \sigma \varepsilon_o}\right), \qquad (5)$$

where ρ is the liquid density, r_o is the radius of static spherical drop, and ε_o is the permitivity of vacuum. The surface charge Q_s can be determined from the levitation condition between two flat parallel electrodes:

$$mg = \frac{Q_s V}{L}, \tag{6}$$

where m is the sample mass, g is the gravitational acceleration, V is the potential difference between the electrodes, and L is the spacing between electrodes. Strictly speaking the shape of a drop which is levitated by an electric force against the gravity deviates from a perfect sphere, and neither the surface charges distributed uniformly. Oscillation of an electrostatically levitated drop in such non-ideal situation has been examined recently by Feng and Beard[15] using multiple parameter perturbation method. Their frequency correction term for axisymmetric n=2 mode is given by

$$\omega_{2c+}^2 = \omega_{osc.}^2 [1 - F(\sigma, q, e)], \tag{7}$$

where ω_{2c+} is the measured frequency ω_{osc} is as defined by Eq. (5), and q and e are defined by

$$q^2 \equiv \frac{Q_s^2}{16\pi^2 r_o^3 \varepsilon_o}, \tag{8}$$

and

$$e^2 \equiv E^2 r_o \varepsilon_o, \tag{9}$$

respectively, where E is the applied electric field. $F(\sigma, q, e)$ in Eq. (7) is defined by

$$F(\sigma, q, e) \equiv \frac{(243.31\sigma^2 - 63.14q^2\sigma + 1.54q^4)e^2}{176\sigma^3 - 120q^2\sigma^2 + 27\sigma q^4 - 2q^6}. \tag{10}$$

6. Summary and Discussions

A new technique which is capable of systematically inducing rotation on a levitated metallic drop was applied for the study of dynamics of rotating charged drops, and for the measurement of surface tension. Helped by the new technique, charged molten tin and aluminum drops were used for the first time to study drop rotation dynamics. Although the drops carried surface charges, the experimental results showed close agreement with the Brown & Scriven's theory if the apparent surface tension (i.e. the resultant surface tension taking into account the effect of surface charges) was used. This experiment showed that surface charges (as high as 24 % for amuminum or 41 % for tin of maximum charges called Rayleigh limit) did not cause any deviation from the prediction. This result is consistant with the previous result obtained from a rotating charged water drop[5]. Good agreement with the prediction was possible only when the condition of solid-body rotation is abided. Under the influence of high level torque the bifurcation of drop shape did not occur at the predicted point, i.e. $\omega_{rot}/\omega_{osc} = 0.559$. Instead, the axi-symmetric branch over-shot the bifurcation point before it transformed into the two-lobed branch. Due to increasing sample position instability as the drops approached the fissioning points, the study of fissioning behavior had to be postponed. An anomalous behavior was observed in a rotating tin which showed strong deviation from the prediction. We speculated that this anomaly was caused by isotope separation under the influence of centrifugal force.

The surface tension measurement approach based on sample rotation was tested using a molten tin drop. The effective oscillation frequency obtained from the rotation experiment near the bifurcation point agreed with the actually measured oscillation frequency within 2 %. This is an encouraging result iin view of the fact that we now have a non-contact method of measuring surface tension of viscous liquids to which the drop oscillation method cannot be applied. Also, this technique will be well utilized in the future development of a non-contact viscosity measurement technique for high viscosity liquids. The area where theses new

techniques may be valuable might be the group of bulk-glass-forming alloys which show viscosity increase more than 12 orders of magnitude during glass-formation processes. Work along this line is being pursued, and the result will be published in a near future.

Aknowledgements:

The authors would like to acknowledge Dr. Paul-Francois Paradis for his help in taking some data, and Mr. D. Barber for the hardware fabrication. This work was carried out at the Jet Propulsion Laboratory, California Institute of Technology, under contract with the National Aeronautics and Space Administration.

References:

[1] W. J. Swiatecki, "The Rotating, Charged or Gravitating Liquid Drop, and Problems in Nuclear Physics and Astronomy," Proc. Int. Coll. on Drops and Bubbles, 1, 52, 1974.

[2] Lord Rayleigh, Phil. Mag. 28, 161, 1914.

[3] S. Chandrasekhar, "The Stability of a Rotating Liquid Drop," Proc. Roy. Soc. London, A 286, 1, 1965.

[4] R. A. Brown and L. E. Scriven, "The Shape and Stability of Rotating Liquid Drops," Proc. R. Soc. Lond. A 371, 331, 1980.

[5] W-K. Rhim, S.K. Chung, and D.D. Elleman, "Experiments on Rotating Charged Liquid Drops," Proc. 3rd International Colloquium on Drops and Bubbles, AIP Conf. Proc. 197: 91, 1988 (ed. T. G. Wang).

[6] A. Biswas, E. W. Leung and E. H. Trinh: "Rotation of ultrasonically levitated glycerol drops", J. Acoust. Soc. Am. 90, 1502-1507, 1991.

[7] T. G. Wang, E. H. Trinh, A. P. Croonquist, and D. D. Elleman, "Shapes of Rotating Free Drops: Spacelab Experimental Results," Phys. Rev. Let. 56, 452, 1986.

[8] W. K. Rhim, S. K. Chung, D. Barber, K. F. Man, G. Gutt, A. Rulison, and R. E. Spjut, "An Electrostatic Levitator for High Temperature Containerless Materials Processing in 1-g," Rev. Sci. Instrum. 64: 2961 (1993).

[9] S. A. Nasar and I. Boldea, Electric Machines (Steady tate Operation), Hemisphere Publishing Corporation 1990

[10] P. L. Alger, Nature of Induction Machine, Gordon and Breach Science Publishers, 1965

[11] T. G. Wang, A. V. Anilkumar, C. P. Lee and K. C. Lin: "Bifurcation of rotating liquid drops: results from USML-1 experiments in Space", J. Fluid Mech. 276, 389-403, 1994.

[12] Lord Rayleigh, Phil. Mag. "On the Equilibrium of Liquid Conducting Masses Charged with Electricity," 14, 184, 1882.

[13] W. K. Rhim, K. Ohsaka, and R. E. Spjut,"A non-contact technique of measuring surface tension and viscosity of molten materials using high temperature electrostatic levitator", Rev. Sci. Instrum. (to be published)

[14] D. D. Elleman, T. G. Wang, and M. Barmatz, "Acoustic Containerless Experiment System: A Non-Contact Surface Tension Measurement," NASA Tech. Memo. 4069, Vol. 2, 557, 1988.

[15] Q. Feng and K. V. Beard: Proc. Roy. Soc. Lond. A. 430, 133, 1990

Table I: Parameters relevant to samples used to obtain Fig. 4

Samples	Aluminum	Tin
Weight (mg)	26.5	27.1
Melting point T_m (°C)	660.5	232
Sample temperature (°C)	705	320
Density at T_m (g/cm^3)	2.38	6.98
Surf. Tension at T_m (mN/m)	914	560
Viscosity at T_m (mP·sec)	2	1.81
Net Electric Charge (nCoul.)	0.445	0.3451
Rayleigh Limit (nCoul.)	1.843	0.851
$Q/Q_{Rayleigh}$ (%)	24.16	41.2

Table II: Parameters relevant to samples used to obtain Fig. 5

Samples	Aluminum	Tin
Weight (mg)	16.8	41.0
Sample Temperature (°C)	790	275
Net Electric Charge (nCoul.)	0.235	0.348
Rayleigh Limit (nCoul.)	1.467	1.003
$Q/Q_{Rayleigh}$ (%)	16	33.4

Figure Captions:

Fig. 1. Top and side views of the electrode assembly used for the present experiment.

Fig. 2. Experimental arrangement which supplied and controlled electric currents supplied to appropriate coils.

Fig. 3. Torque versus normalized sample rotation frequency measured using an aluminum sphere at three different applied currents.

Fig. 4. Normalized drop size versus normalized drop rotation frequency of both molten tin and aluminum drops are compared with the theoretical curves obtained by Brown and Scriven.

Fig. 5. A new but smaller aluminum drop was rotated and compared with the predicted curves. Use of higher torque might be the cause of those points past the predicted bifurcation point. Those specifically marked points showes drops shapes as shown in Fig. 6.

Fig. 6. Drop shapes of rotating aluminum drop of Fig. 5 each of which specifically marked using same alphabet.

Fig. 7. Anomalous behavior of a rotaing tin drop when it was kept for two hours at a two lobed shape.

Fig. 8. The shape of the anomalous tin (of Fig. 7) when it finally came to rest.

Fig. 9. Evolution of shapes of rotaing aluminum and tin drops were plotted in terms of R_{max}/R_{min} versus $\omega_{rot}/\omega_{osc}$.

Fig. 10. The result after the normalization of tdata points shown in Fig. 9.

Fig. 11. The Apparant oscillation frequencies obtained based on the drop rotation at different rotation frequency are compared with the directly measured oscillation frequency of the same drop.

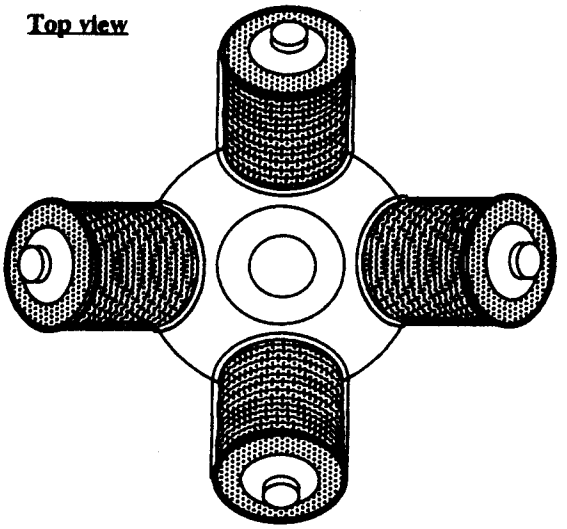
Top view

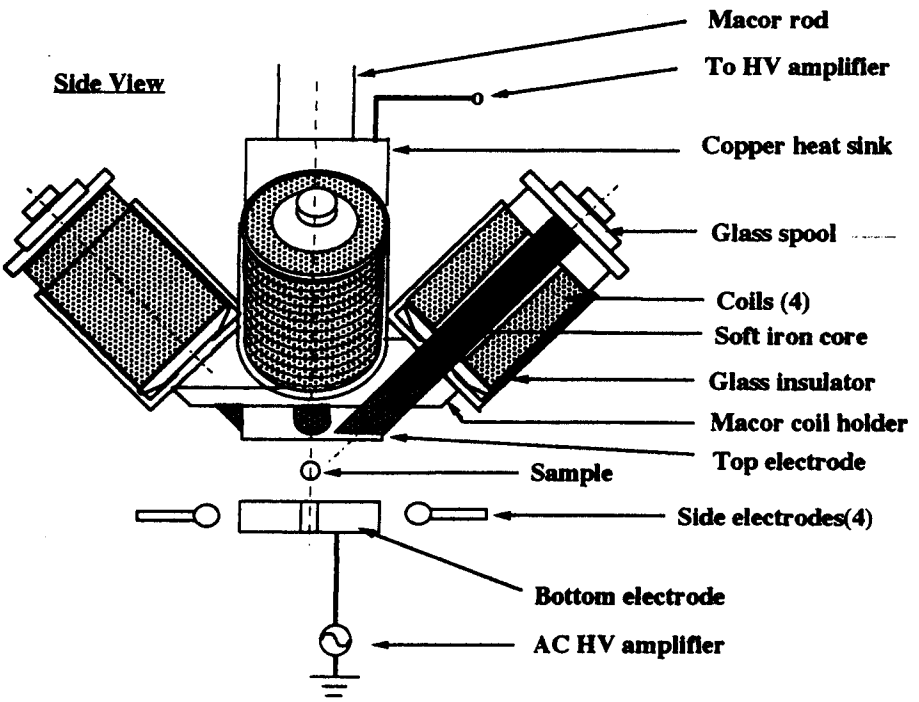
Side View
Macor rod
To HV amplifier
Copper heat sink
Glass spool
Coils (4)
Soft iron core
Glass insulator
Macor coil holder
Top electrode
Sample
Side electrodes(4)
Bottom electrode
AC HV amplifier

Fig. 1

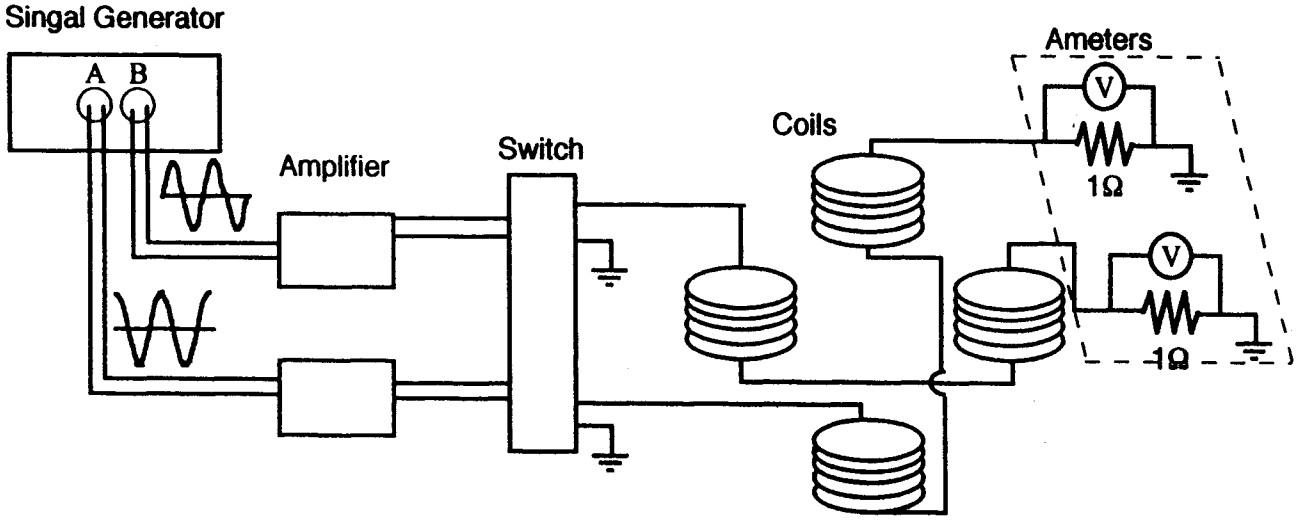
Singal Generator
A
B
Amplifier
Switch
Coils
Ameters
V
1Ω
V
1Ω

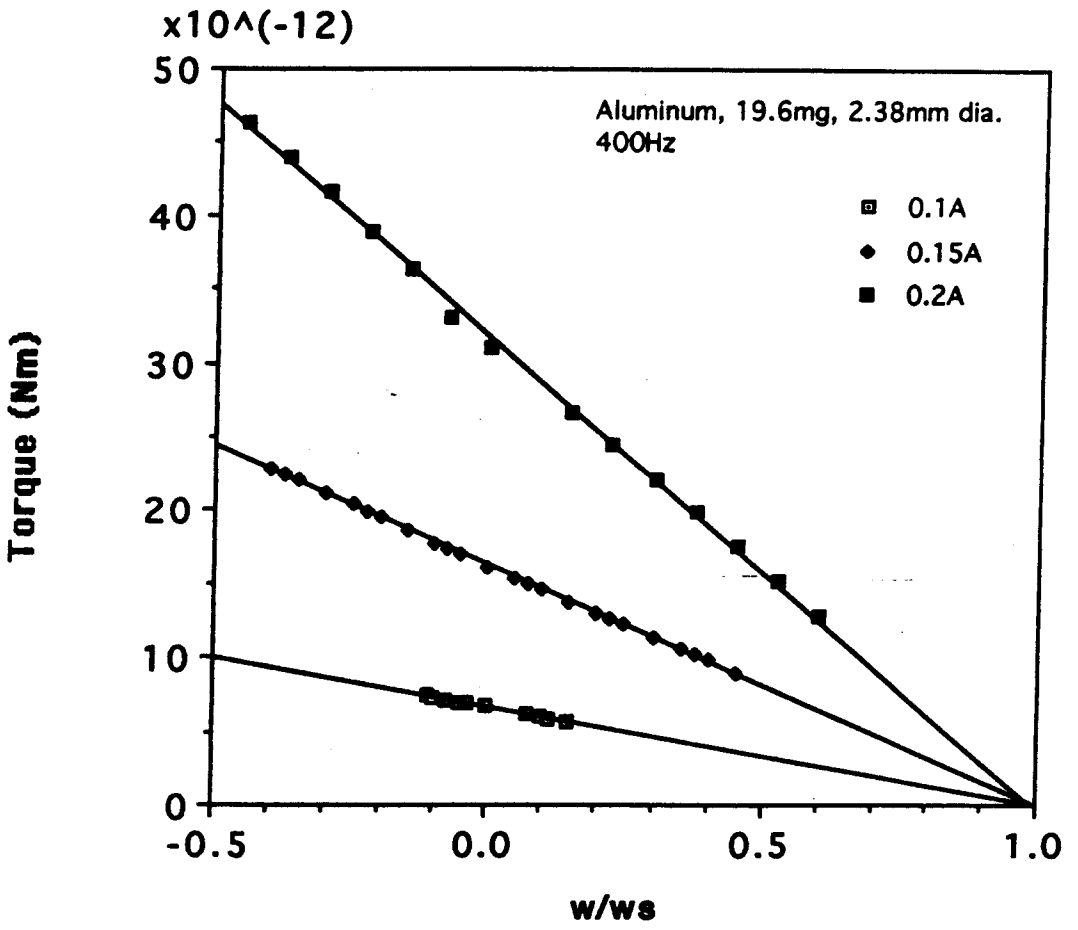
x10^(-12)
50
40
30
20
10
0
Torque (Nm)
Aluminum, 19.6mg, 2.38mm dia.
400Hz
0.1A
0.15A
0.2A
-0.5
0.0
0.5
1.0
w/ws

Fig 3

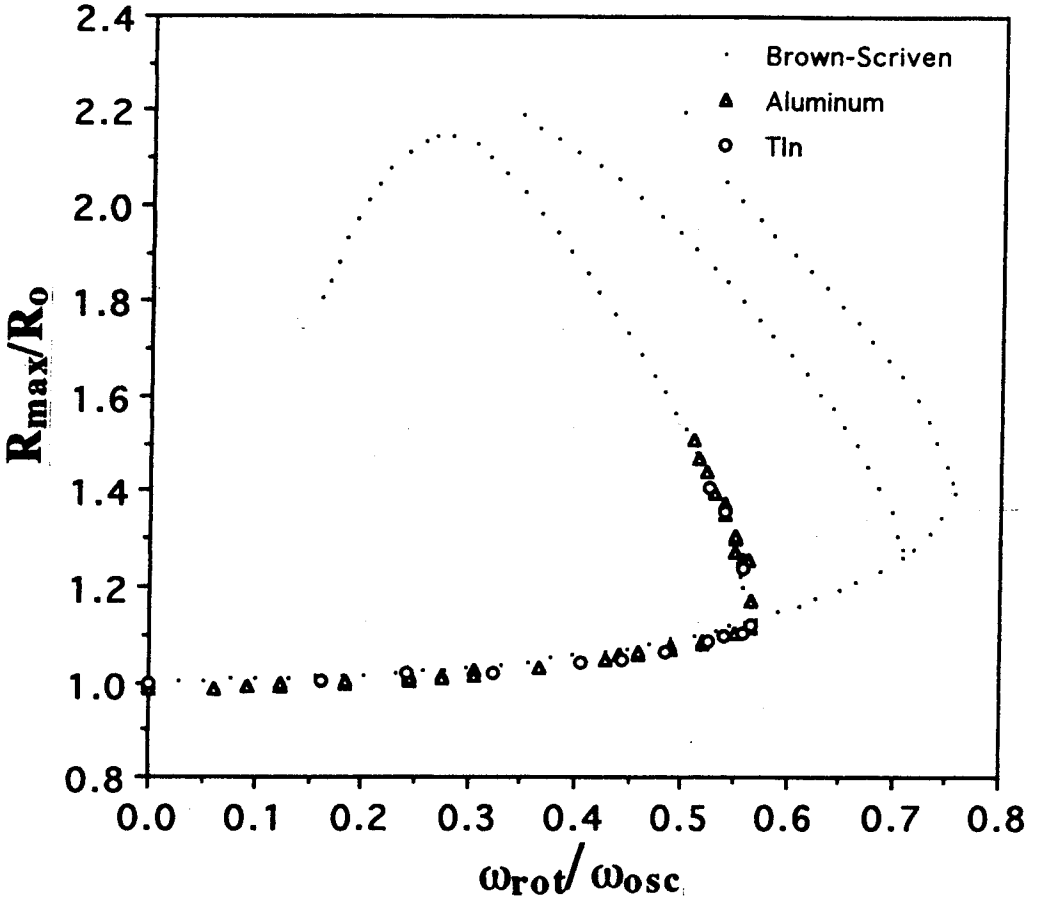

Al. 26.5 mg 705°C (0.95%) -7 KV (d = 12 mm

Tin: 27.1 mg ~~260°C~~ 320°C ($\frac{1.698 - 1.692}{1.692} \times 100\%$ = 0.35%)

-9.08 KV

d = 12 mm

(no record)

Fig. X

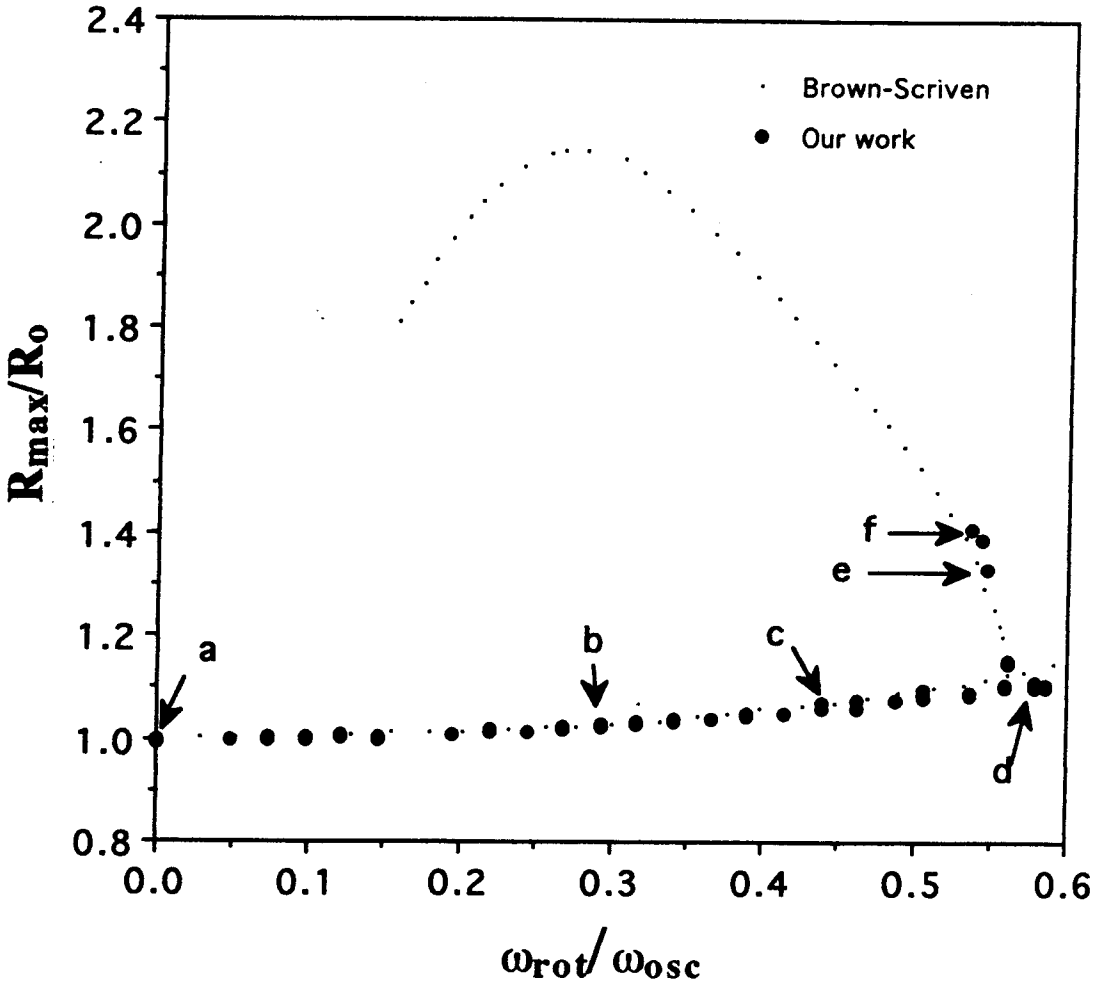
2.4
2.2
2.0
1.8
1.6
1.4
1.2
1.0
0.8
0.0
0.1
0.2
0.3
0.4
0.5
0.6
Brown-Scriven
Our work
a
b
c
d
e
f
R_{max}/R_o
$\omega_{rot}/\omega_{osc}$

F.# 5

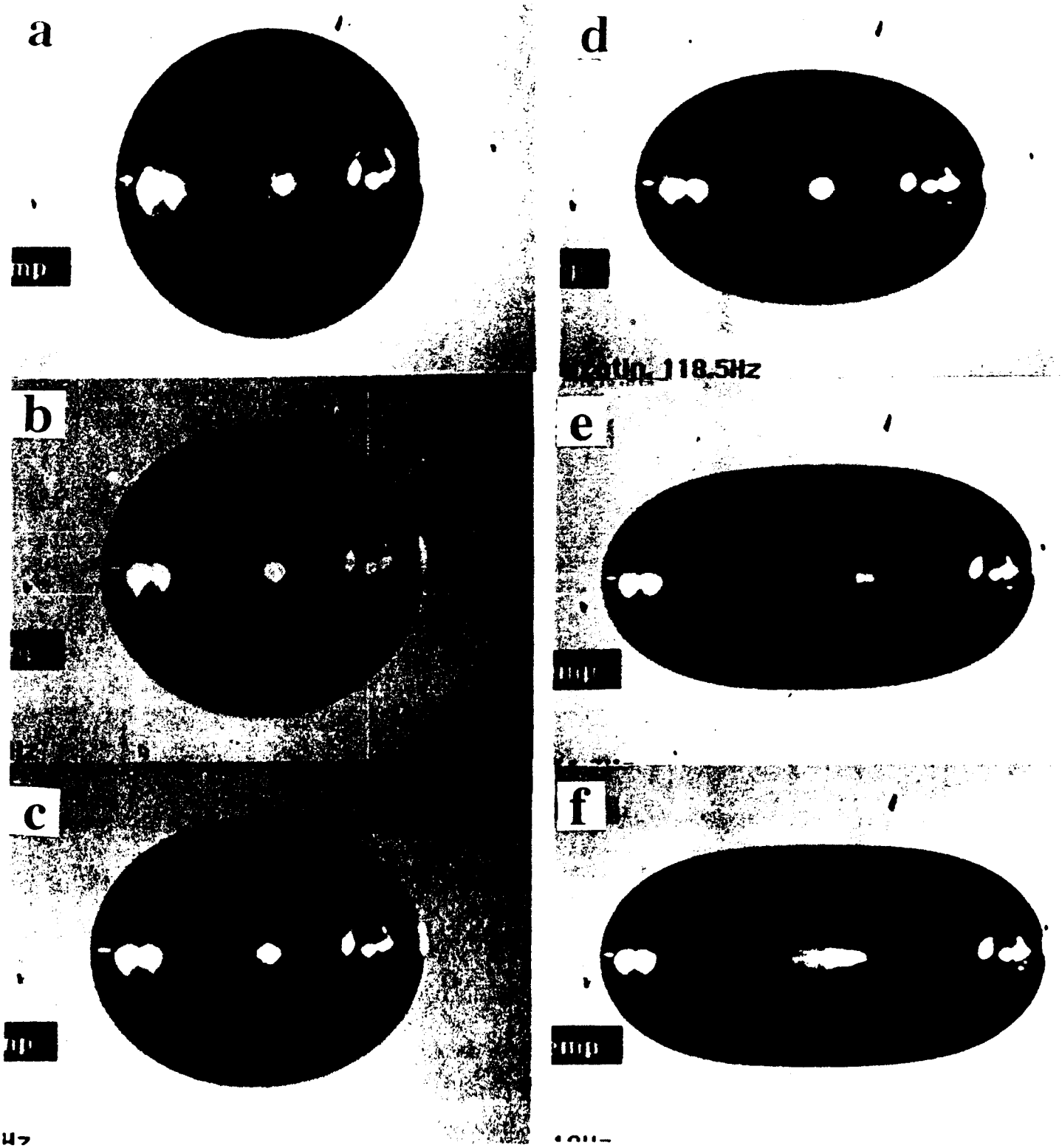

F8

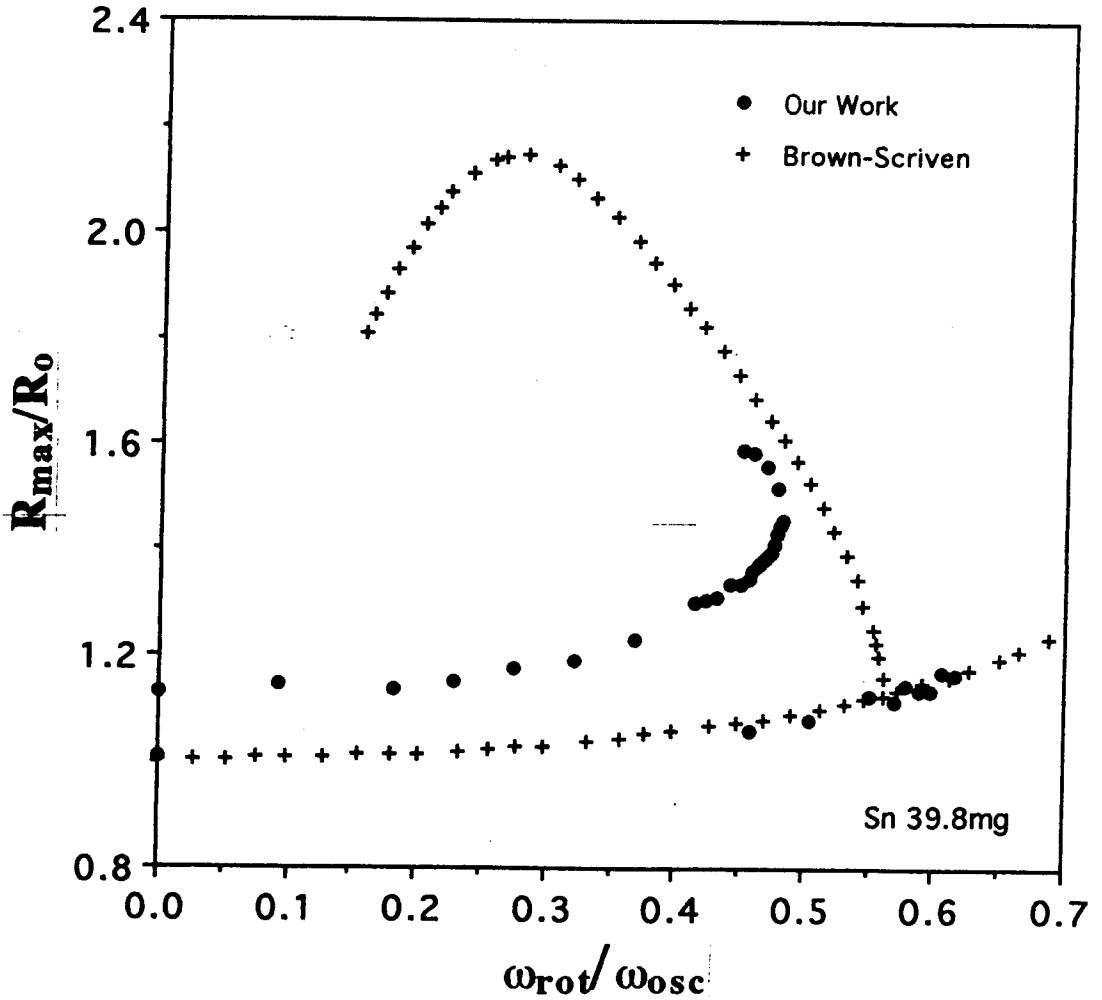
2.4
2.0
1.6
1.2
0.8
0.0
0.1
0.2
0.3
0.4
0.5
0.6
0.7
Rmax/Ro
ωrot/ ωosc
Our Work
Brown-Scriven
Sn 39.8mg

Fig 7

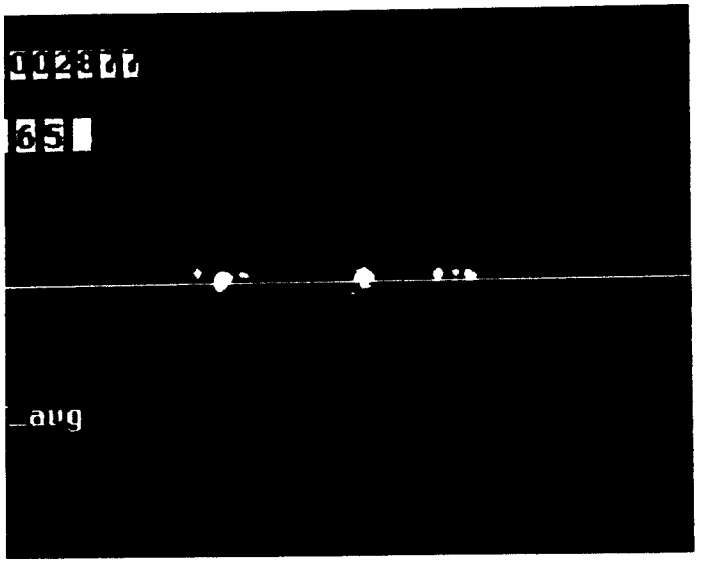

Fig 8

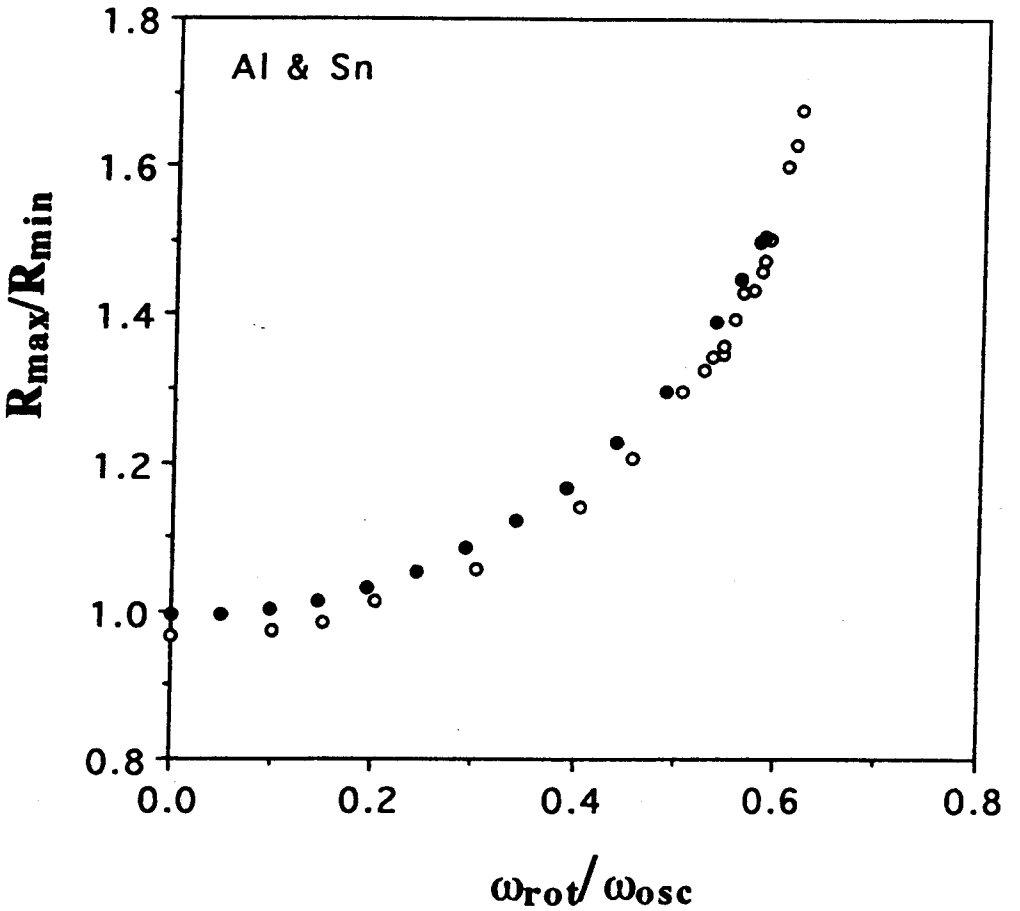

Al = 16,8 mg 26KV d=10 mm

S_n = 41 mg, 275°C, 11.5KV, d=10 mm

F58

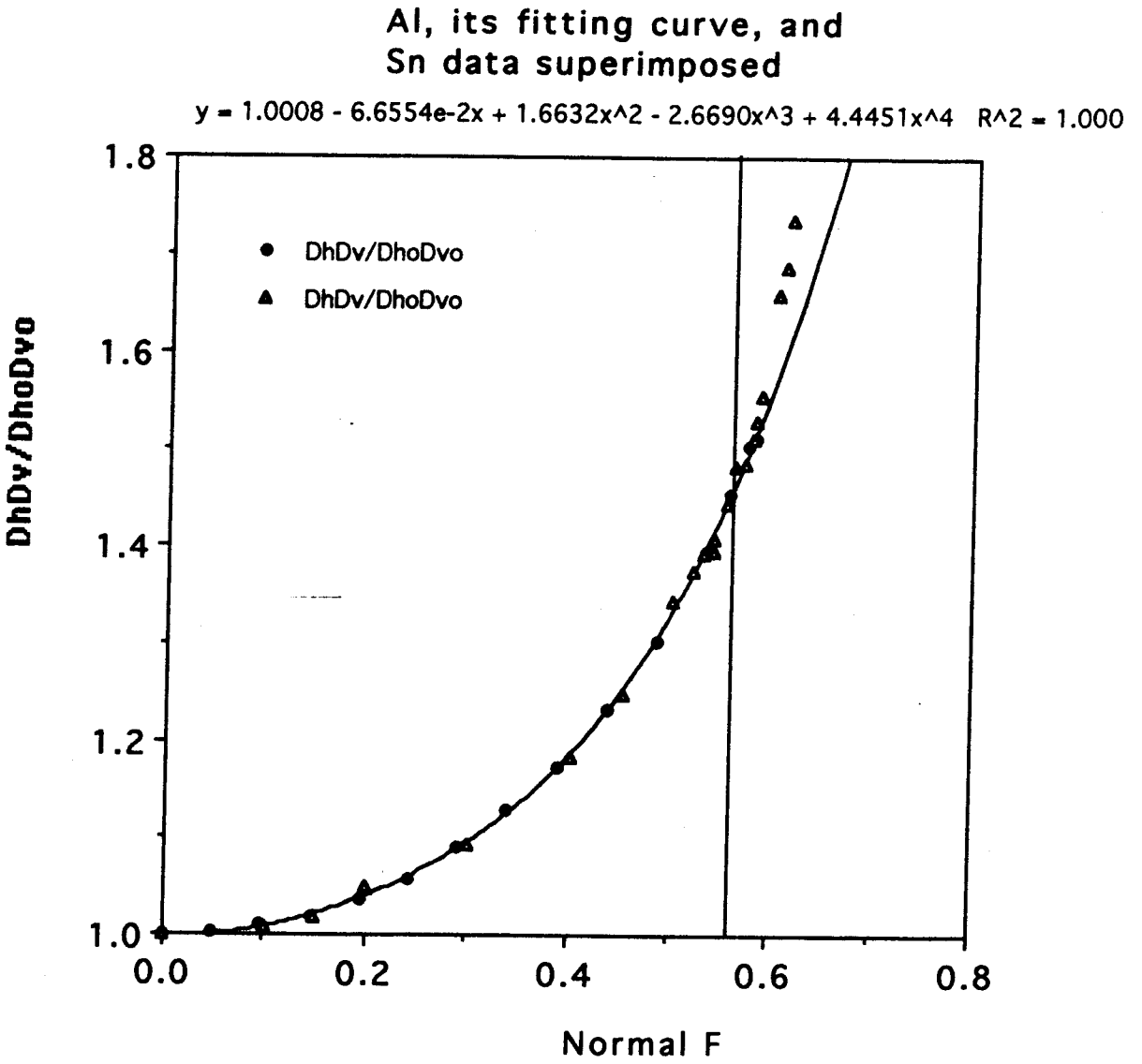
Al, its fitting curve, and
Sn data superimposed
y = 1.0008 - 6.6554e-2x + 1.6632x^2 - 2.6690x^3 + 4.4451x^4 R^2 = 1.000
DhDv/DhoDvo
DhDv/DhoDvo
DhDv/DhoDvo
1.8
1.6
1.4
1.2
1.0
0.0
0.2
0.4
0.6
0.8
Normal F

Fig. 1c

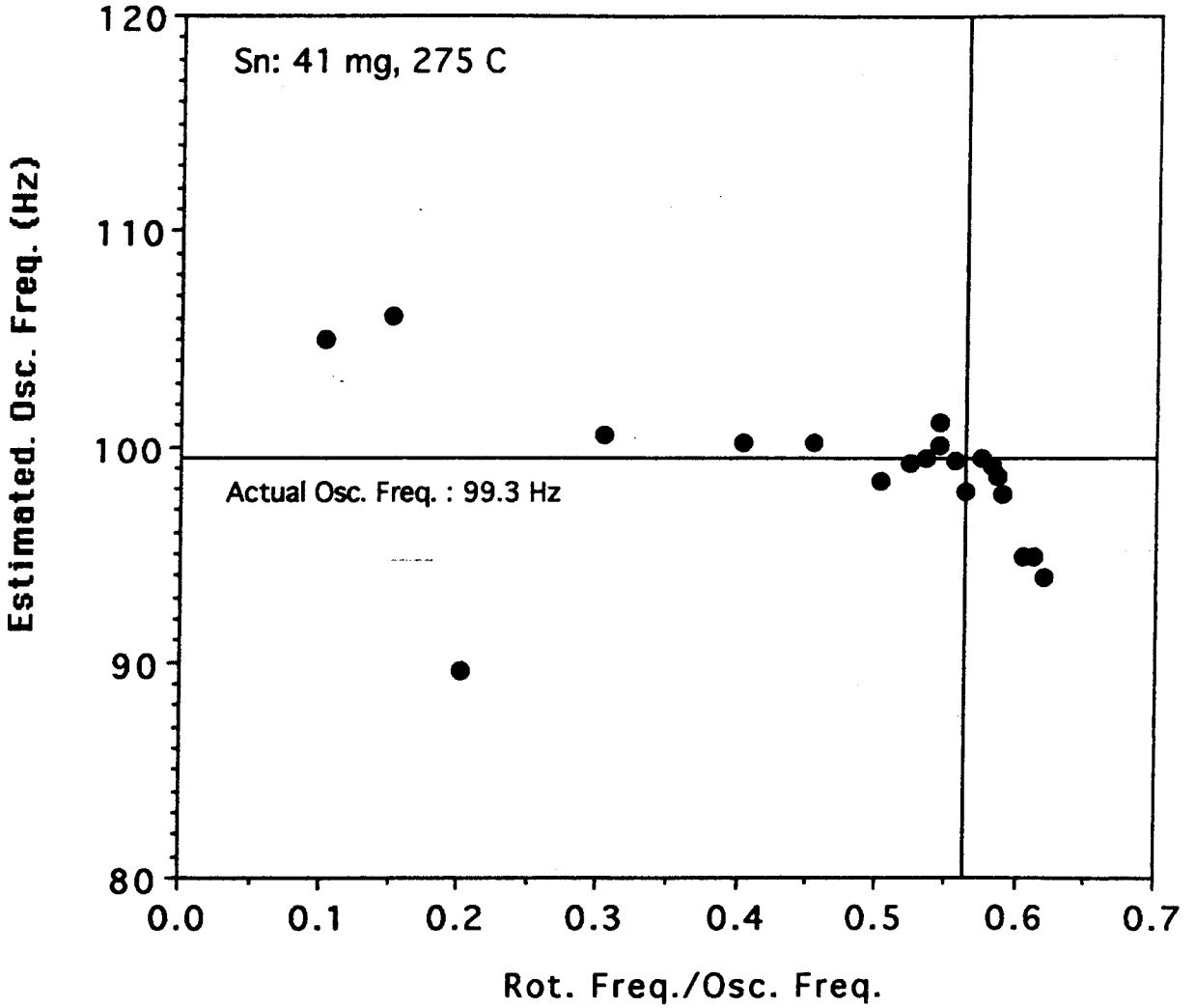
Sn: 41 mg, 275 C
Actual Osc. Freq. : 99.3 Hz
Estimated. Osc. Freq. (Hz)
120
110
100
90
80
0.0
0.1
0.2
0.3
0.4
0.5
0.6
0.7
Rot. Freq./Osc. Freq.

Fig. 11